COMPDYN 2013
4th ECCOMAS Thematic Conference on
Computational Methods in Structural Dynamics and Earthquake Engineering
M. Papadrakakis, N.D.Lagaros, V. Plevris (eds.)
Kos Island, Greece, 12–14 June 2013

# SIMULATION OF STRUCTURAL POUNDING WITH THE SEARS IMPACT MODEL

**Sushil Khatiwada[1], Nawawi Chouw[2], and Tam Larkin[2]**

[1] The University of Auckland
Private Bag 92019
Auckland 1142, New Zealand
e-mail: skha178@aucklanduni.ac.nz

[2] The University of Auckland
n.chouw@auckland.ac.nz
t.larkin@auckland.ac.nz

**Keywords:** Adjacent structures, Building pounding, Distributed mass impact, Sears model.

**Abstract.** *Seismic pounding affects some buildings and bridge spans with insufficient expansion joints. During pounding, structures exert repeated hammer- like blows on adjacent structures or structural elements which causes a range of effects from minor cosmetic spalling to major structural damage in buildings while bridge spans may be unseated.*
*Several methods have been proposed for numerical simulations of pounding. The most common method is the contact element model, where a link is introduced between the pounding masses to allow simulation of the contact force. Unfortunately, most of these models have been developed based on the collision of spheres, idealized as concentrated masses, while the pounding structures have distributed masses. These models also suffer from uncertainties regarding the stiffness of the links and the duration of contact as well as the amount of energy lost during contact. Some studies have also proposed a pounding model as an impact between two bars whose response is governed by stress wave propagation. These models can predict the energy loss during impact and the duration of impact but have a major drawback that the strain in the bars rises instantaneously to a finite value, which results in an infinite acceleration. Similarly, they can predict a negative value of the coefficient of restitution which makes no sense from a physical stand-point.*
*This paper proposes a quasi-empirical impact mechanism for simulation of structural pounding. The model includes the effects of both the contact surface properties and the cross-sectional properties of the bars. The pounding force is calculated from the deformation and stiffness at the contact location, but the duration of contact and the development of the local deformation is a function many factors for which a parametric analysis is presented. Finally, an example of a building pounding analysis with the proposed model is provided.*

## 1 INTRODUCTION

Building pounding has been observed in many urban earthquakes. The most publicized occurrence was in Mexico City in 1985, where pounding was identified as the cause of 15% of all collapsed buildings [1]. Recently, many instances of pounding were observed during the 2011 Christchurch earthquake [2]. Pounding is defined as the collision between structures or parts of structures, for instance, between bridge decks, due to the at-rest separation being insufficient to accommodate the relative seismic displacement. The relative displacement is due to the out-of-phase motion between affected structures or structural elements. Such motion can be caused by the differing dynamic properties of the structures, foundation flexibility effects, or the spatial variability of ground motion in bridge piers [3].

Pounding has long been identified as a recurring hazard. Several solution methods and models have been produced to simulate pounding analytically. All these models rely on time history analysis of the structures. In all models, the structures are assumed to vibrate independently of each other, until the relative closing motion is less than a predefined gap. When the gap closes, and the structures come into contact, the methods differ in the treatment of the impact. Some of the early studies on pounding treated the impact with the laws of stereomechanics [4]. The loss of mechanical energy is incorporated by a predetermined coefficient of restitution, *e*, which is defined as the ratio of relative separation velocity to relative approach velocity of the colliding masses. The post-impact velocities of the masses can be calculated once the masses and initial velocities are known.

A major drawback of stereomechanics is the need to interrupt the time history analysis at every contact to update the velocities of the masses, which necessitates renewed calculation of all the coefficients used in the considered time window. This method is generally not included in commercial finite element software. Thus, the 'impact element method' was developed where an elastic or viscoelastic link is introduced with an accompanying gap at possible contact locations (Figure 1). The link is activated when there is contact, and deactivated at separation. The impact force is a function of the stiffness and damping of the impact element. The damping of the impact element is calculated so that the post-impact velocity is same as that calculated from stereomechanics. The inclusion and exclusion of the impact element's properties in the damping and stiffness matrices in time history analysis is supported by most of the commercial finite element software, so this method is more common than the stereomechanical method.

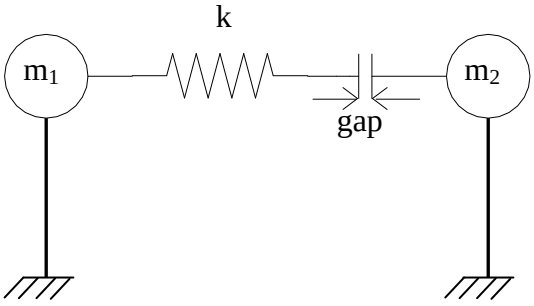


Figure 1: Lumped mass model with impact element.

The previous two methods idealize the building slabs or bridge decks that collide as point masses i.e. the whole bodies undergo a velocity change simultaneously. In reality, the structural members have sufficient length to introduce a finite time-lag for the stress waves to travel from impact locations to the other ends of the members. Malhotra [5] demonstrated the effects of the propagation of stress waves on the pounding of bridge decks. It was shown that

for the decks of identical material and cross sectional properties, the resulting coefficient of restitution was given by the ratio of the length of the shorter deck to the longer deck. Thus, even for an elastic contact, there was apparent energy loss due to unequal length of the decks. While the contact duration is a function of colliding masses and contact stiffness in the impact element method, it only depends on the material properties and length of the bodies in stress wave methods.

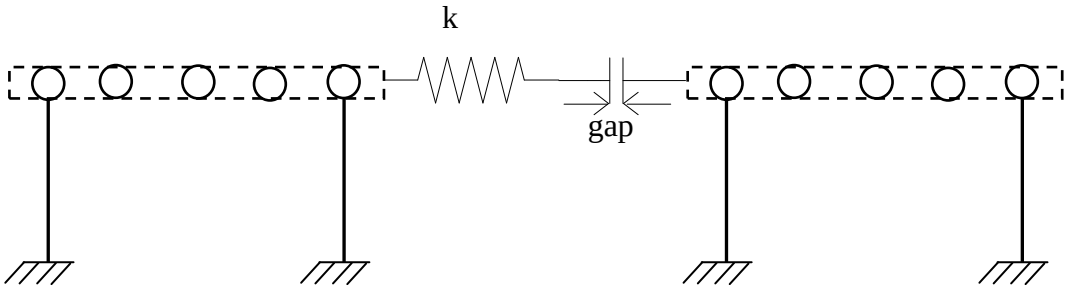


Figure 2: Distributed mass model of impact.

Malhotra [5] proposed that the coefficient of restitution may be determined from the ratio of lengths and a method similar to stereomechanics to analyze the pounding of bridges. Watanabe and Kawashima [6] proved that finite element software can be employed to simulate the stress wave propagation in colliding bridge decks. The impacting members were discretized as shown in Figure 2. The authors proposed that the stiffness of the link should be equal to the stiffness of the adjoining segments for the best agreement with wave theory. Cole *et al*. [7] extended the model to the analysis of building pounding. The authors derived a coefficient of restitution for colliding members with different material and geometrical properties by considering the first modes of axial vibration of building slabs. It was shown that finite element discretization of colliding building slabs produced similar results.

The methods based on wave theory of impact also have some significant drawbacks. For instance, both Malhotra [5] and Cole *et al.* [7] predict a constant duration of contact for two given bodies, but experiments have shown that the duration depends upon the relative impact velocity [8]. The impact force from distributed mass simulations showed significant positive and negative variation about the value predicted by wave theory [6, 7]. Another concern is the abrupt changes in velocity resulting in a nearly instantaneous imposition of strain, which can be construed as nearly infinite acceleration at the contact location. Finally, the relationships derived from wave theory for the general cases of contact have been found to result in a negative coefficient of restitution which is at variance with the laws of physics [7].

Thus building pounding has been modeled either as the impact of lumped masses, where only the local surface geometries are instrumental in the analysis; or as wave propagation effects in longitudinal bars which are defined by the cross-sectional properties of the diaphragm. Experiments have shown that the impact force of two bars depends on a combination of the local and cross-sectional properties [9]. Wagstaff [8] showed that the point mass contact can better predict the impact of short bars with rounded ends, while wave theory was found to be more effective for contact forces of longer bars. None of the models that have been proposed for the simulation of pounding can combine the effect of both these situations.

A composite contact model was first proposed by Sears [10] in which the contact force is determined by Hertz theory but the state of the distant portions of the bars is given by wave theory. The current article proposes the adaptation of the Sears impact model for structural

pounding simulations. A parametric study of the behavior of the model is presented. Finally, a simulation of pounding between a pair of one story buildings is shown.

## 2 THEORY OF THE SEARS IMPACT MODEL

The theory has been adapted from Goldsmith [9] and is discussed with respect to the contact of two circular bars with rounded ends, as shown in Figure 3. Sears proposed that there is a zone of compression adjacent to the contact surface which extends to the vertical plane containing point P1 on the left bar and to the vertical plane containing point P2 on the right bar. The impact force is generated by the compression of this zone. As the contact occurs, stress waves propagate away from the location of contact in both bars. As the stress waves reach a section, its velocity undergoes a more gradual change depending on the magnitude of the force, while the distant sections keep moving with the initial velocities. Initially the force is insufficient to stop the compression, so the compression keeps increasing. After a certain time, the stresses in the compression zone are high enough to cause a gradual release of stress at the contact zone and eventually separation.

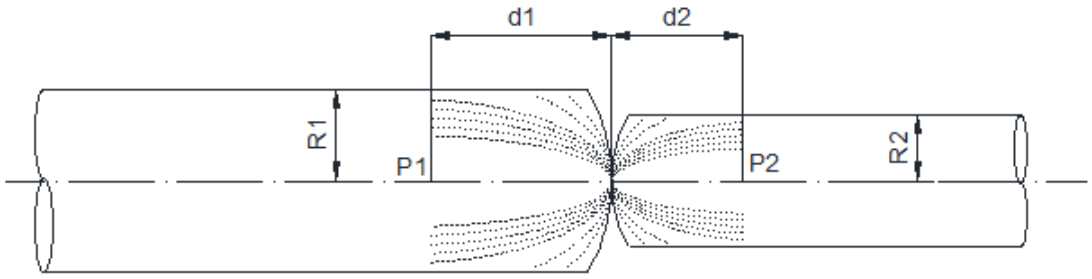


Figure 3: Collision of two circular bars with rounded ends.

If the two bars are moving with velocities $v_1$ and $v_2$, where subscript 1 refers to the left bar and 2 refers to the right bar, the compression $\delta$ at any time $t$ before the stress wave reaches points $P_i$ is given by,

$$\delta = v_1 t - v_2 t \tag{1}$$

Because of the deformation, a force $F$ develops at the contact location given by

$$F = k\,\delta^{3/2} \tag{2}$$

where $k$ is the stiffness of contact. For the spherical contact surfaces, according to the Hertz contact law,

$$k = \frac{4}{3\pi(h_1 + h_2)} \left( \frac{r_1 r_2}{r_1 + r_2} \right)^{1/2} \tag{3}$$

where, $r_1$ and $r_2$ are the radii of the rounded ends,

$h_1$ and $h_2$ are given by,

$$h_i = \frac{1 - \mu_i^2}{\pi E_i} \tag{4}$$

where $\mu_i$ and $E_i$ are the Poisson's ratio and Young's modulus of the $i^{th}$ bar.

Sears [10] proposed the length of the deformation zone as,

$$d_i = R_i \left[ \sqrt{\frac{3}{2}} + \frac{1}{\sqrt{6}} (1+\mu)(3-2\mu) \right] \tag{5}$$

where $R_i$ is the radius of the i$^{th}$ bar.

The stress wave reaches point $P_i$ at $t = d_i/c_i$ where $c_{i\ is}$ the compression wave propagation velocity in $i^{th}$ bar given by $c_i = \sqrt{E_i / \rho_i}$ where $\rho_i$ is the density of the i$^{th}$ bar. The expression for compressive deformation becomes

$$\delta = v_1 t - v_2 t - \frac{1}{\rho_1 A_1 c_1} \int_0^t F_{\left\langle t - \frac{d_1}{c_1} \right\rangle} dt - \frac{1}{\rho_2 A_2 c_2} \int_0^t F_{\left\langle t - \frac{d_2}{c_2} \right\rangle} dt \tag{6}$$

where $A_1$ and $A_2$ are the cross-sectional areas of the bars and the force $F$ becomes zero when the expression within the conical brackets is zero.

The stress waves will travel to the far end of the bars and undergo reflection. When the reflected waves reach points $P_i$, Equation 6 becomes

$$\delta = v_1 t - v_2 t - \frac{1}{\rho_1 A_1 c_1} \int_0^t \left[ F_{\left\langle t - \frac{d_1}{c_1} \right\rangle} + F_{\left\langle t - \frac{d_1 + l_1}{c_1} \right\rangle} \right] dt - \frac{1}{\rho_2 A_2 c_2} \int_0^t \left[ F_{\left\langle t - \frac{d2}{c2} \right\rangle} + F_{\left\langle t - \frac{d_2 + l_2}{c_2} \right\rangle} \right] dt \tag{7}$$

where $l_i$ is the length of the i$^{th}$ bar outside the compression zone.

If separation does not occur, the waves will reach the contact end and once again be reflected, leading to a new term being added to the right hand side of Equation 7. For each successive reflection from either end in either bar, a new expression is similarly added. The expression for deformation can be generalized as,

$$\begin{aligned} \delta = v_1 t - v_2 t &- \frac{1}{\rho_1 A_1 c_1} \int_0^t \left[ F_{\left\langle t - \frac{d_1}{c_1} \right\rangle} + F_{\left\langle t - \frac{d_1 + l_1}{c_1} \right\rangle} + F_{\left\langle t - \frac{d_1 + 2l_1}{c_1} \right\rangle} + F_{\left\langle t - \frac{2d_1 + 2l_1}{c_1} \right\rangle} + \ldots \right] dt \\ &- \frac{1}{\rho_2 A_2 c_2} \int_0^t \left[ F_{\left\langle t - \frac{d2}{c2} \right\rangle} + F_{\left\langle t - \frac{d_2 + 2l_2}{c_2} \right\rangle} + F_{\left\langle t - \frac{d_2 + 2l_2}{c2} \right\rangle} + F_{\left\langle t - \frac{2d_2 + 2l_2}{c_2} \right\rangle} + \ldots \right] dt \end{aligned} \tag{8}$$

The reflective terms will be added to Equation 8 until $\delta$ becomes zero or negative. When this occurs, the two bars separate and the contact force vanishes. Equation 8 can be solved for incremental time steps to find the resultant impact force time history.

## 3 PARAMETRIC INVESTIGATIONS OF THE SEARS MODEL

The impact force from the Sears model is affected by a multitude of parameters whose effects are not readily apparent. Hence, a parametric investigation of a simple impact of two circular rods is presented here. A circular steel rod of diameter 0.1 m is assumed to strike another rod of the same diameter at a relative impact velocity of 1 m/s. The impacted end of the first bar has a rounded end of diameter 0.1 m, while the impacted end of the second bar is flat. The simulations are carried out with a time step of 1 microsecond except in the case of

very stiff contact elements which required a time step of 0.1 microseconds. The length of the bars is first varied to best reflect the effect of that parameter. A discussion of the effects of other parameters follows.

### 3.1 Effect of length of bars

Changes in bar lengths produced surprising changes in the force time history (Figure 4). It readily becomes apparent that for a given cross-sectional area, there is an upper limit for the maximum impact force, no matter what the lengths of the participating bars. For bars with identical cross-sectional and material properties, the limit is same as that obtained in wave theory [5, 7], i.e. $0.5\rho Ac(v_1\text{-}v_2)$. For shorter bars, this maximum force may never be attained. For longer bars, after a relatively short rise time, the force remains at the maximum for a large part of contact time, followed by a steep attenuation to zero.

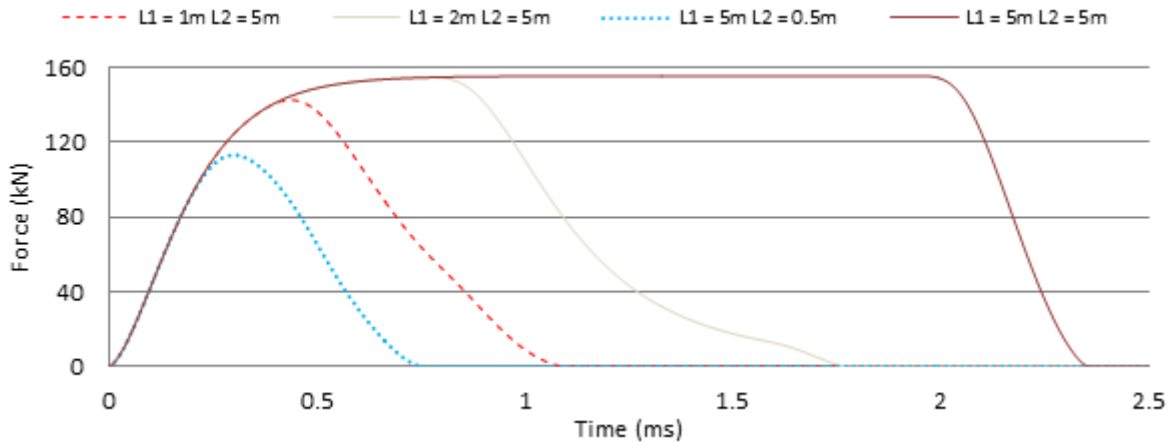


Figure 4: Impact force for different bar lengths.

Figure 5 shows the force time histories produced by Sears, Hertz and wave propagation models. The force from Hertz's model is based on Equation 2 while the force from wave theory, according to Cole *et al*. [7] equals $0.5\rho Ac(v_1\text{-}v_2)$ over a duration obtained by dividing twice the length of the short bar by the compression wave velocity in the bars. The results prove that the Sears model for impact force is governed by the mechanics at the point of contact for short bars and distributed mass effects for longer bars.

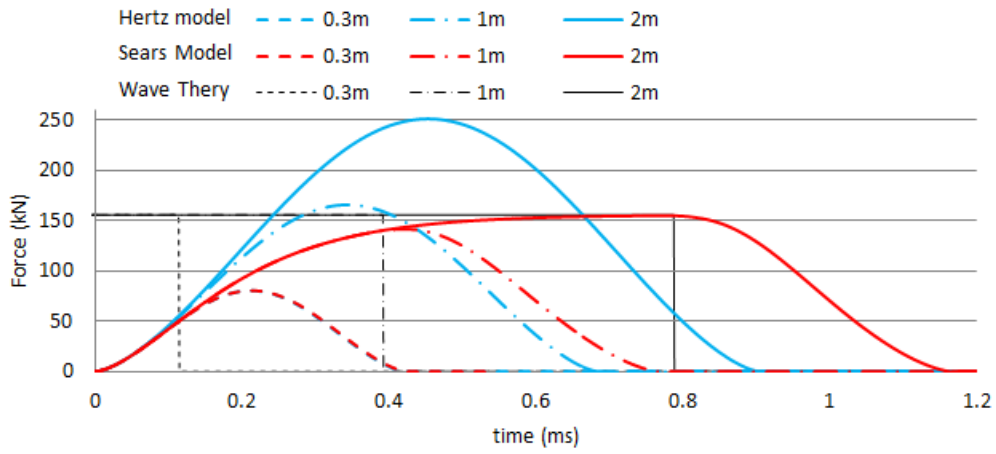

Figure 5: Impact force from various models for bars of equal length and cross section.

The final velocities of the bars were calculated by equating the impulse of the impact force with the change in momentum of the bars. The calculated effective coefficients of restitution are shown in Figure 6. In Hertz contact, the coefficient of restitution has to be predetermined, while in the wave theory it is equal to the ratio of the lengths of the short bar to the long bar. Thus, when at the contact location no energy loss is assumed in these computations, the Hertz model would give a coefficient of restitution as 1. It was seen that while the Sears model was also affected by the ratio of the lengths, it depended equally upon the length of the shorter bars. For very short bars, the coefficient approached unity but for longer bars, it became similar to wave theory. When both the bars are very long, the results become indistinguishable with those from wave propagation theory.

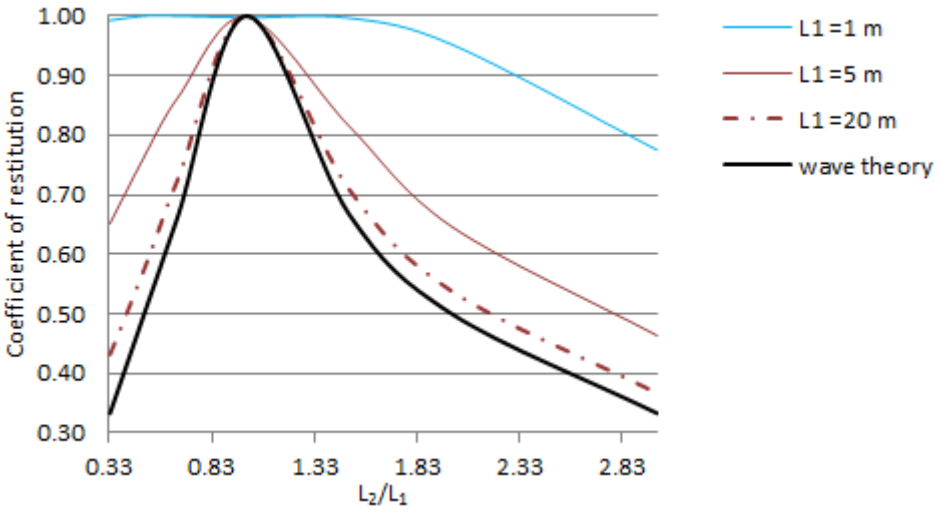


Figure 6: Coefficient of restitution for impact of unequal bars.

### 3.2 Effect of relative impact velocity

An increase in the relative impact velocity between bars of unequal length resulted in the duration of contact decreasing and *vice versa* (Figure 7). The decrease in contact duration was accompanied by a decrease in coefficient of restitution, see Figure 7. Thus, for higher impact velocities, more energy was trapped in the internal vibration of the bars. The impact of short bars was affected more than that of the longer bars. Thus, an increase in the relative impact velocity shifts the impact behavior more towards wave theory.

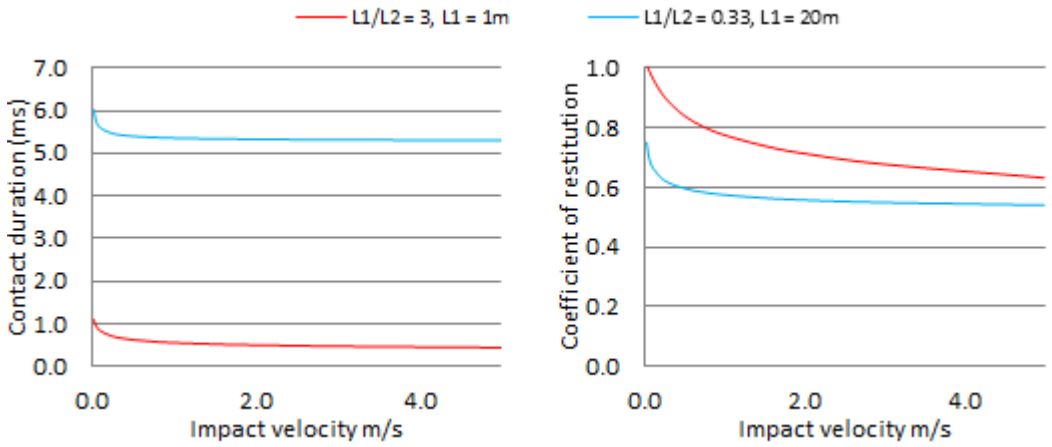


Figure 7: Variation of (a) contact duration, and (b) coefficient of restitution with relative impact velocity

### 3.3 Effect of mass

This section describes the outcome of analyses using the Sears model and varying the contributing mass. The participating mass could be increased in two ways, by putting a superimposed mass on the bars or by increasing the cross-sectional area. For simplicity, the superimposed mass was assumed to be uniformly distributed over the length of the bars. It was observed that the behavior was same for both these cases. The duration of contact and coefficient of restitution both increased with increasing mass. Thus, the contact behavior is shifted toward that of a lumped mass model by an increase in mass. The effective coefficient of restitution was always positive, even where the mass and length ratio produced negative values in methods from wave theory [7].

### 3.4 Effect of contact stiffness

The contact stiffness was varied by changing the diameter of the spherical cap. It was observed that the contact duration as well as coefficient of restitution decreased with increasing stiffness (larger dome diameter). Both as a ratio, and in seconds, the decrease in contact duration was significantly more for shorter bar collisions than for longer bars. With sufficiently high contact stiffness, all of the impacts generated a force almost identical to the wave theory, while the softer contact skewed the behavior towards a lumped mass collision.

### 3.5 Effect of the length of compression zone

The effect of the variation in the length of the compression zone $d_i$ was investigated because it is based on assumptions [10]. The length $d_i$ was varied from a hundredth of the calculated value to ten times as much. Surprisingly the results showed that the contact force was not very sensitive to $d_i$. The maximum variation observed was 4% when a hundredth of the default value was employed. Thus, despite the considerable effort expended to calculate $d_i$ in the original derivation of theory, the behavior of the model is very little affected by this factor.

### 3.6 Effect of material properties

Figure 8 shows the effect of material variation. First the participating steel bars were replaced by M20 concrete of the same dimensions. It was observed that, due to the reduction in stiffness and mass, the contacts force is softer and the duration is longer. A uniformly distributed mass was placed on the concrete bars to allow comparison of the results for concrete and steel bars of equal mass. It can be seen that, the increased mass shifted the contact proper-

ties toward lumped mass impact, and a maximum limiting force is never reached. The effective coefficient of restitution did not change for the change in materials, but did change significantly with additional mass.

From the results presented, it is obvious that the Sears model is capable of simulating both lumped mass and distributed mass impacts, as well as the intermediate transition zone. The buildings undergoing pounding can be of different shapes, sizes, material or utility with differing supports. When modeled as a lumped mass contact, the effective coefficient of restitution can vary widely from the predetermined coefficient. Similarly, application of wave theory may significantly underestimate the effective coefficient of restitution for low velocity or heavy mass contacts.

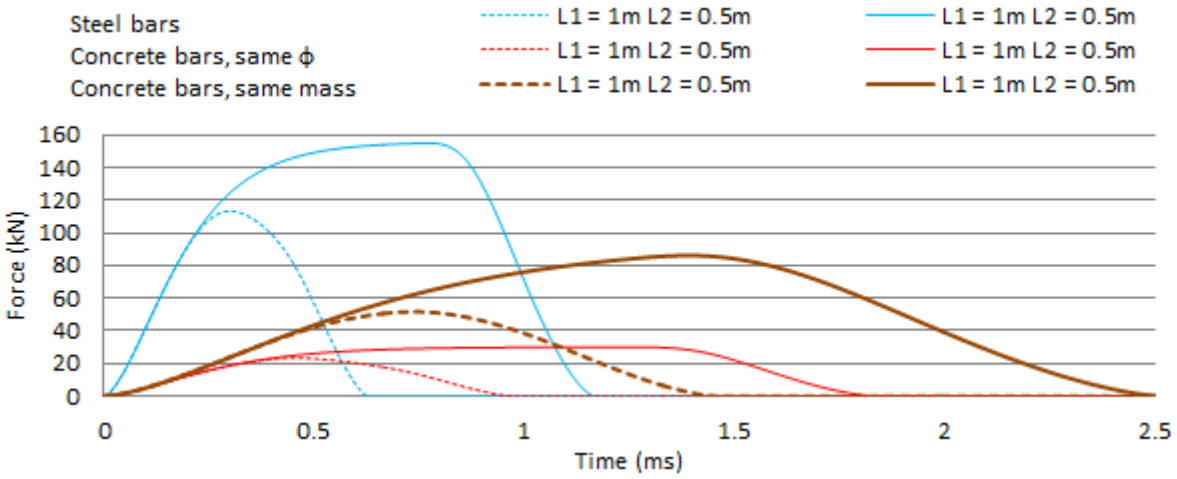


Figure 8: Effect of material properties on the impact force

## 4 BUILDING POUNDING SIMULATION

The implementation of the proposed model in building pounding simulation is complex. It is not possible to pre-calculate the coefficient of restitution as suggested by Malhotra [5], since the coefficient does not remain constant. Creation of an equivalent lump mass model, as suggested by Cole *et al.* [7] is also not advisable as the contact duration cannot be predetermined.

An integral part of the formulation presented here is the Hertz theory for the stiffness of spheres in contact (Equation 2 and subsequently Equations 3 and 4). The Hertz theory has certain assumptions which are only valid for curved surfaces, and it cannot be applied for contact of plane surfaces [9]. Since most of the structural pounding problems involve contact between two flat surfaces, the current authors postulate that the linear force-deformation relationship (Equation 10) is more suitable.

$$F = k_L \, \delta; \qquad \delta > 0 \tag{10}$$

where $k_L$ is the linear stiffness of the collision element and $\delta$ is the longitudinal deformation of the contact zone.

Contact stiffness $k_L$ is calculated as $[EA/(L/n)]$ when $n = d/L$ is the ratio of the length of the deformation zone to the length of the whole bar. The contact element stiffness $k_L$ cannot be determined currently with any degree of certainty. It was found that the stiffness calculated assuming the total length of the slab or beam as a single element tended to produce a very soft contact which results in the contact force not reaching the limiting force, $F_{max}$. If only a part of the bars was assumed to participate in the development of impact force, the contact dura-

tion became shorter and the limiting force was achieved. Figure 9 shows the effect of increasing value of *n* for contact between two concrete slabs of dimension 10 m x 8 m x 0.15m, with impact velocity 1 m/s. Stiffness $k_L$ is calculated as [EA/(L/n)] where n is the number of discrete elements. It was observed that the rise time of the force, and total contact time decreased as *n* was increased. Large scale experiments to measure the effective contact zone of diaphragms will need to be carried out to forecast the contact stiffness with certainty. For the analysis presented here, the zone of axial deformation of slab is assumed to be a tenth of the length of the stiffer slab.

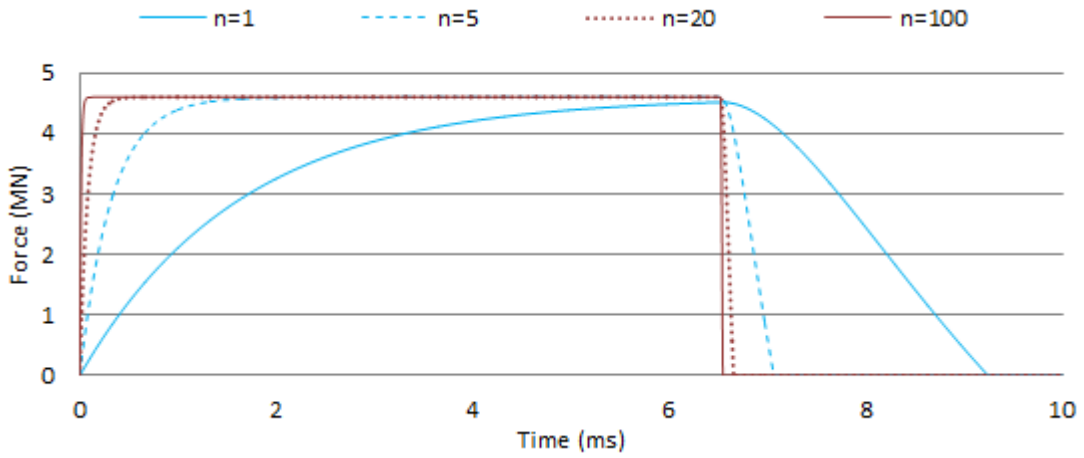


Figure 9: Variation in impact force with the increasing ratio of total length to the length of compression zone

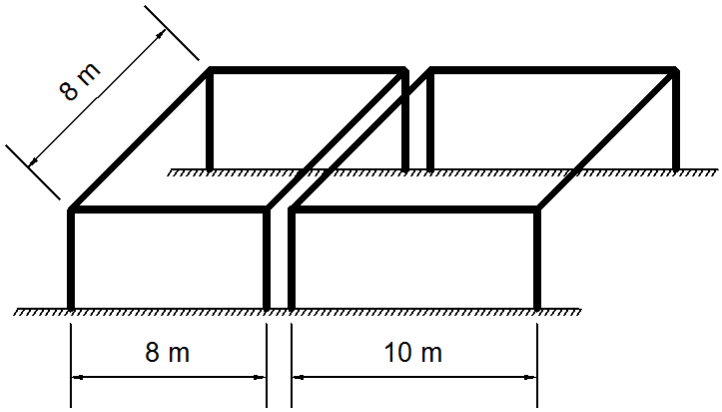


Figure 10: One-story buildings for pounding simulation.

| Properties | Left Building | Right Building |
|---|---|---|
| Floor height | 4 m | 4 m |
| Slab thickness | 0.15 m | 0.15 m |
| Building stiffness | 1.16 x $10^7$ N/m | 7.11 x $10^6$ N/m |
| Seismic mass | 36,000 kg | 45,000 kg |
| Natural period | 0.35 s | 0.5 s |

Table 1: Properties of the buildings subjected to pounding.

The buildings shown in Figure 10 were subjected to eight seconds of El Centro ground motion (Figure 11). Table 1 shows the relevant properties of the buildings. The seismic weight of

the building was assumed to be uniformly distributed over the whole area of the roof. The at-rest separation was 1 mm. The contact stiffness was calculated to be 15 GN/m. The roofs were modeled as single uniaxial members for the calculation of impact force, while the buildings were idealized as single degree of freedom structures for time history analysis. The displacement responses of the building with and without pounding are presented in Figure 12.

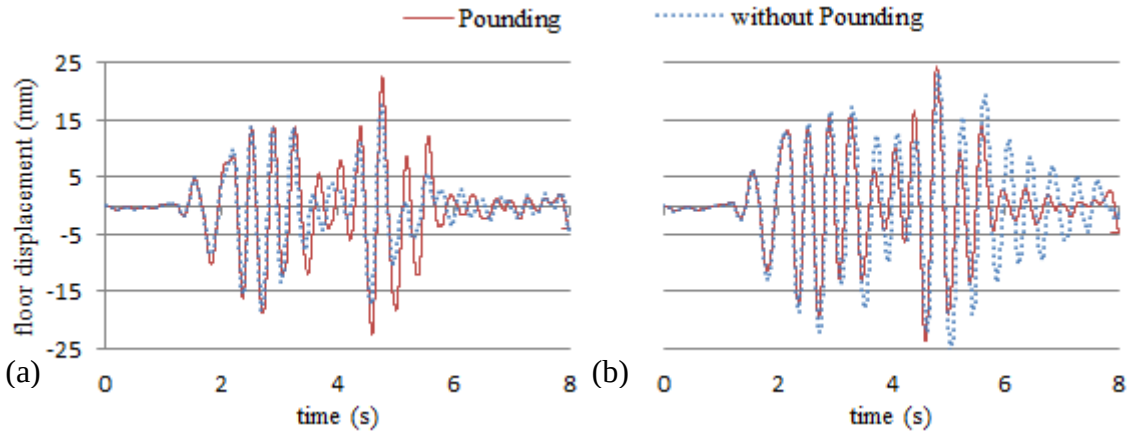


Figure 12: displacement time histories with and without pounding (a) left building and (b) right building.

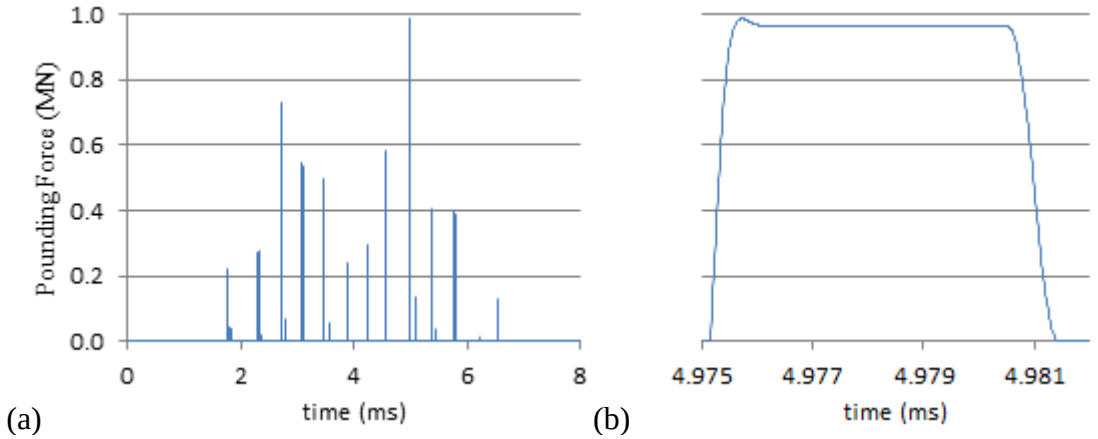


Figure 13: (a) Pounding forces throughout the simulation and (b) Pounding force during thirteenth impact.

Figure 13a shows the pounding forces generated throughout the simulation. Nineteen contacts occurred in total. The time history of force during the strongest impact is presented in figure 13b. The contact force resembled that from wave theory due to the stiff contact element. When the deformation zone was assumed to be longer, the contact softened, and the impact force shifted toward Hertzian contact for which the results are not shown here.

## 5 CONCLUSIONS

- A method that can incorporate the behavior of distributed mass as well as lumped mass models is proposed for building pounding. The impact force has a finite rise time, as opposed to the instantaneous peak force in wave theory. While the force time-history has a flat plateau after it reaches a maximum value which is dependent on the density and Young's modulus of elasticity of the material as well as the cross sectional area and velocity of the bodies. This plateau can only occur in a lumped mass model if there is plastic deformation at the contact location.

- A parametric study of the model was presented. It was observed that the contact could behave more like that of point masses or distributed masses depending on the values of the parameters involved. An increase in impact velocity shortened the contact duration and produced impact forces similar to that in wave theory. An increase in masses of the bodies shifted the contact behavior toward lumped mass impact. Wave propagation was the predominant mode when the bodies were longer while the contact of shorter bodies was governed by lumped mass effects. Finally, if the bars of softer material (concrete) were loaded with the same mass, the lumped mass behavior becomes more significant.
- The effective coefficient of restitution was found to be dependent upon the length ratio of the bars as in wave theory. For elastic contact of two bars of equal lengths the coefficient of restitution was always one, but for unequal lengths it was governed by almost all the parameters studied. The coefficient of restitution approached unity for short bars while for longer bars it approached the ratio of the length of the shorter bar to that of longer bar. Thus, lumped mass models can significantly over-estimate the effective coefficient of restitution while models based on wave theory can underestimate it equally severely.
- The Sears model was derived for impact of curved ends. A modification is proposed for building pounding analysis, where a linear force deformation equation is adopted instead of the Hertz model to calculate the impact force at the contact location. This requires the length of the deformation zone to be determined. The effect of this length is also presented. Unfortunately, the current state of the art is insufficient to predict this with any certainty.
- Finally, a procedure for the implementation of the Sears model in the simulation of building pounding is outlined. The contact zone was assumed to be a tenth of the length of the stiffer slab, and the results from a sample analysis are presented. It was observed that the simulated forces were similar to the wave propagation model, but contained definite rise and fall durations. The oscillations observed in the force time history from previous published studies on distributed mass modeling were absent.
- In summary, the Sears model is recommended for implementation in building pounding analysis as it can combine into one methodology two currently used models as well as rectify some weaknesses in both. Large scale testing of the impact between slabs is also recommended to determine the force development at the contact zone.

## ACKNOWLEDGEMENTS:

The first author is deeply indebted to The University of Auckland for the grant of the University of Auckland International Doctoral Scholarship.

## REFERENCES

[1] E. Rosenblueth, R. Meli, The 1985 earthquake: causes and effects in Mexico City. *Concrete International*, **8**, 23-34, 1986.

[2] Chouw, N., Hao, H. (2012). Pounding damage to structures in the 2011 Christchurch earthquake. *International Journal of Protective Structures*, 3**(**2), 123-139.

[3] B, Li, K. Bi, N. Chouw, J.W. Butterworth, H. Hao, Experimental investigation of spatially varying effect of ground motions on bridge pounding. *Earthquake Engineering and Structural Dynamics*, **41**, 1959-1976, 2012.

[4] C.J. Athanassiadou, G.G. Penelis, A.J. Kappos, Seismic response of adjacent buildings with similar or different dynamic characteristics. *Earthquake Spectra*, **10**, 293-317, 1994.

[5] P.K. Malhotra, Dynamics of seismic pounding at expansion joints of concrete bridges. *ASCE Journal of Engineering Mechanics*, **124**, 794–802, 1998.

[6] G. Watanabe, K. Kawashima, Numerical simulation of pounding of bridge decks. *Thirteenth World Conference on Earthquake Engineering*, Vancouver, B.C. Canada, August 1-6, 2004.

[7] G.L. Cole, R.P. Dhakal, A.J. Carr, D.K. Bull, The effect of diaphragm wave propagation on the analysis of pounding structures. *4th ECCOMAS Thematic Conference on Computational Methods in Structural Dynamics and Earthquake Engineering (COMPDYN 2009)*, Rhodes, Greece, June 22-24, 2009.

[8] J.E.P. Wagstaff, Experiments on the Duration of Impacts, Mainly of Bars with Rounded Ends, in Elucidationof the Elastic Theory. *Proceedings of the Royal Society of London. Series A, Containing Papers of aMathematical and Physical Character*, **105**, 544-570, 1924.

[9] W. Goldsmith. *Impact: the theory and physical behaviour of colliding solids, Dover ed*. Dover, 2001.

[10] J.E. Sears, On longitudinal impact of metal rods II. *Transactions of the Cambridge Physical society*, **21**, 49-106, 1912.